

AFRL-SR-BL-TR-02-

intaining the
for reducing
A 22202-
y a currently

20020402 087

AIR FORCE OFFICE OF SCIENTIFIC RESEARCH (AFOSR)
NOTICE OF TRANSMITTAL DTIC. THIS TECHNICAL REPORT
HAS BEEN REVIEWED AND IS APPROVED FOR PUBLIC RELEASE
LAW AFR 190-12. DISTRIBUTION IS UNLIMITED

MAR 15 2002

**PROPAGATING POTENTIAL DISTURBANCES
IN TURBOMACHINERY**

FINAL REPORT

**Eric J. Jumper
Department of Aerospace and Mechanical Engineering
University of Notre Dame
Notre Dame, IN 46556**

**Performance Period
1 May 1999 – 30 November 2001**

**AFOSR Grant F49620-99-1-0251
March 2002**

TABLE OF CONTENTS

	Page
Standard Form 298	i
Table of Contents	ii
Executive Summary	iii
I. Introduction	1
Sources of Potential Disturbances	2
Why Study Potential Disturbances in the Notre Dame Cascade	4
II. The Trailing-Edge Interaction	5
III. Use of von Karman Vortex Shedding from Circular Cylinders for Unsteady Disturbance Sources	7
IV. Overcoming the Shortcomings of the Earlier Study	8
Experimental Parameters	8
V. Early Results of the Present Research (or Drowning While Standing Knee Deep in the Stream of Happiness)	9
AMMi Transducer Results	9
Kulite Transducer Results	11
Fundamental Amplitude	13
Normalized First-Harmonic Amplitude	13
Cylinder Vortex Shedding	15
VI. In Search of the Perfect Potential Disturbance (or the Creation of In-Phase Forcing-Cylinder Shedding)	16
VII. Discussion and Conclusions	18
Acknowledgement/Disclaimer	18
References	18
Appendix A: Mid-1990 Notre Dame Cascade Results	21
Appendix B: Grant and P.I. Information	27

EXECUTIVE SUMMARY

This final report describes the work performed under an AFOSR Grant, Propagating Potential Disturbances in Turbomachinery. There is an almost universal presumption that the major cause of unsteady forcing in a turbine engine is due to vortical disturbances. Vortical disturbances are created as momentum-deficit wakes emanating from turbine-engine components and are convected with the flow downstream from their origin, subsequently interacting with engine components farther downstream in the engine. On the other hand, aerodynamic distortion of the flow within an engine due to the presence of engine components and their bound circulation have been known to be present; but, their role as a source for unsteady forcing of engine components has been generally assumed to be of secondary importance to that caused by vortical disturbances. These aerodynamic flow distortions, which may be steady or unsteady, are referred to as *potential disturbances*. If these disturbances are unsteady in the frame of a component, and if the flow is compressible, then these disturbances propagate and, unlike vortical disturbances, they may propagate both up and down stream. Within the last half decade, unsteady-surface-pressure responses measured on sharp-trailing-edged vanes positioned upstream of potential disturbance sources have been shown to be as large in amplitude as, and in some case larger in amplitude than, the response due to comparable vortical disturbances. What is more, the upstream-propagating potential disturbances appear to produce trailing-edge-biased loading. In the case of at least one study performed for a specially-instrumented IGV positioned in the potential-disturbance field ahead of an F109 fan, the elicited trailing-edge-biased response was alarmingly large. It is a fact that 56% of all fighter aircraft mishaps in the Air Force between 1982 and 1996 have been attributed to engine High-Cycle Fatigue (HCF), which by definition are due to unexpected, unsteady forcing. Since forcing due to potential disturbances has been largely, though not exclusively, ignored, it seems imperative that a detailed study to document both the unsteady velocity field associated with an unambiguous potential disturbance, and its vane-interaction response be undertaken; this research was directed toward that task. If these data are obtained, theories might be devised to explain these large interaction responses and these theories can be incorporated into predictions of aerodynamic forcing in turbine engines.

The present effort relied on successful cascade studies performed in an unsteady compressible cascade at Notre Dame in the mid 1990's. The results of those studies are summarized in *Appendix A* of this report; it was, in fact, those mid-1990 studies that led to a very-successful and ongoing series of studies in the F109 turbofan engine that was referred to above. In the present study, changes in the design of the cascade were made in an attempt to overcome the shortcomings of the earlier studies; in particular, initially, only a single unloaded vane was located at the center of the duct. Further, this vane had sufficient thickness to accommodate surface-pressure measurements back to 93% chord, whereas the earlier study could only accommodate measurements back to the 80% chord. The symmetric airfoil arrangement also allowed for higher spatial resolution in the measurements by alternating chord locations from one side to the other of the vane. In the earlier studies, von Karman shedding from cylindrical rods placed downstream of loaded vanes were used as the potential-disturbance sources for the studies; these rods proved to be perfect potential-disturbance generators, all shedding in phase with no requirement for any control mechanisms. As is described in the body of this report, relatively late in our present study we realized that in our new cascade configuration, the rods no longer shed in phase. Although response data was collected and again relatively large amplitudes were measured, such out-of-phase shedding caused the pressure response data to be too ambiguous to be interpretable. Further, unlike the earlier studies, where only a fundamental and a harmonic were required to disassemble the response into interpretable response, the response on the vane in the present study contained a large amount of structure. This structure was such that, although in many cases the unsteady surface pressure response increased toward the trailing edge, when processed using methods used in the earlier studies, the apparent trend in the response was to decrease toward the trailing edge.

Toward the end of the present effort, we concentrated on attempting to phase lock the shedding on the forcing rods in order to produce potential disturbances of quality comparable to the earlier studies. Even though the funding for this effort has now ended, Notre Dame is committed to continue the effort to create interpretable potential disturbances.

PROPAGATING POTENTIAL DISTURBANCES IN TURBOMACHINERY

F49620-99-1-0251

Eric J. Jumper

Department of Aerospace and Mechanical Engineering
University of Notre Dame, Notre Dame, Indiana

I. INTRODUCTION

As will be discussed later in this report, our effort ran into a number of difficulties in producing a clean potential disturbance. These difficulties were totally unexpected, as will be described below; however, they set the work back by enough time that we were unable to accomplish all the goals of the program. In this *Introduction*, I would like to lay out the case that the original goals of the work are still extremely important to understanding what we have now shown to be a first-order effect in unsteady forcing in turbine engines, *upstream-propagating potential disturbances*. There seems to be some misunderstanding as to the contributions that Notre Dame has made in identifying the importance of this first-order effect and this, in part, may be due to a general confusion about the various types of potential-disturbance interactions that can occur, these being primarily differentiated by the sources of the disturbances; so, in this *Introduction*, I will attempt to categorize the various types of potential-disturbance interactions that can occur. It is important to note that, depending on the environment, a number of these interactions can occur simultaneously and it is precisely the obscuration that is introduced by this simultaneity that we have attempted to avoid in this research effort and why I continue to argue for continuation of this work.

In general, unsteady flow in turbine engines occurs because of the interaction between moving rotor blades and stationary stator vanes, as well as the presence of flow-distorting structures and inlet distortions. The unsteadiness in the flow interacts with the blades and vanes to cause an unsteady pressure response on their surfaces, which, in turn, can couple into the structure of the component; this coupling may eventually lead to structural failure. The importance of being able to properly account for (predict) the nature of both the forcing field and its coupled response is underscored by the fact that 56% of all fighter aircraft mishaps in the Air Force between 1982 and 1996 have been attributed to engine High-Cycle Fatigue (HCF) [Ref. 1].

Based on a review of the literature prior to 1995, the main contributor to unsteady pressure response in turbine engines was attributed to vortical gusts associated with the wakes from upstream components that subsequently interact with the downstream blades/vanes as the disturbances convect with the flow. Although potential disturbances are treated throughout the literature, ever since the initial papers associated with von Karman and Sears, there was a general, though not total, consensus that these disturbances were of second-order importance. This consensus began to develop with one of the earliest papers on inter-stage interactions; the paper was by Kemp and Sears

[Ref. 2]. The Kemp and Sears analysis was for incompressible flow and treated only potential disturbances; because the flow was incompressible, the potential fields due to the rotors and stators were instantly felt throughout the field, and so, in this sense, did not propagate. The wakes were included only to the extent that the shed circulation, carried downstream with the flow, caused a delay in the lift and moment build up in the, by then well understood, Theodorsen-function-type delay that depends on reduced frequency, k . Further, the analysis used classical thin airfoil theory, so that the trailing-edge Kutta condition was enforced, i.e., no singularity was allowed at the trailing edges of the airfoils.

The conclusions of the paper were interesting in that the upstream stator's unsteady lift (integrated unsteady pressure field) due to the presence of the downstream rotor was approximately three times larger than the unsteady lift on the rotor due to the upstream stator. When the spacing between the stator's trailing-edge plane and the rotor's leading-edge plane was 0.2 rotor-chord, the unsteady lift of the 45°-turning-stator was approximately 15% of the steady lift for a reduced frequency of one; this unsteady lift decayed exponentially with separation distance, decaying to less than 5% of the steady lift by 0.6 chord separation. A reduced frequency of 2 gave a response which was approximately $\frac{1}{4}$ that of $k = 1$ for 0.2 chord separation, and well less than 1% by 0.6 chord; higher harmonics had successively lower effect and decayed even more rapidly. It should also be noted that because of the use of thin airfoil theory, the unsteady lift acted through the $\frac{1}{4}$ chord, and, by necessity, had a zero pressure difference across the trailing edge. From this paper onward, it has been generally assumed that potential disturbances at blade-passage reduced frequencies (order 4 and higher) must produce negligible response on upstream components that, in any case, must act through the aerodynamic center with no particular enhanced unsteady loading near the trailing edge. The rapid decay in the disturbance with increasing reduced-frequency harmonics might also be reached by looking at steady cascade analyses for incompressible flow and noting the rapid decay of the spatial harmonic content in the potential field both up and downstream of the leading and trailing edges of the vane row, respectively. To some degree or another, others have looked at potential disturbances experimentally and computationally, either affirming the negligible influence of potential disturbances or questioning the wisdom of this commonly-accepted presumption. The lack of general consensus over the impact of potential disturbances on unsteady pressure response may have been due to a misunderstanding of the differing character and origin of various sources of potential disturbances and a tendency to lump all potential disturbances into one pigeonhole.

Sources of Potential Disturbances. Potential disturbances are associated with inviscid flow distortions due to the presence of bodies in the flow and their bound circulation. These flow distortions extend outward from the bodies, and are generally known/assumed to decay relatively rapidly, decaying exponentially over distances of roughly the body's dimension. Although potential disturbances can extend both upstream and downstream from the body, for the purpose of this discussion, I will only address the upstream influence of the potential flow distortions. Even with the exponential decay, in the case of a stationary engine component, such as a support strut, for example, its potential field may have sufficient dimension so that it extends upstream into the flow field of an upstream rotor, even extending through a stator row positioned between the

strut and the rotor. Since the strut is fixed in the engine frame, its potential field appears unsteady only to the rotor, which cuts through this otherwise steady field. This case is depicted in the upper left of Figure 1. In this case, the potential field does not radiate (propagate), since the rotor intersects the field everywhere at the same time. This case has been studied at VPI [see for example Ref. 3], and their research has been instrumental in understanding and relieving fan vibratory forcing due to struts in the bypass ducts. Although Ng et. al. showed that a strut with a sharp trailing edge also experiences unsteady bound circulation, their approach to the strut problem considered the strut's potential field to be a steady, stationary flow distortion.

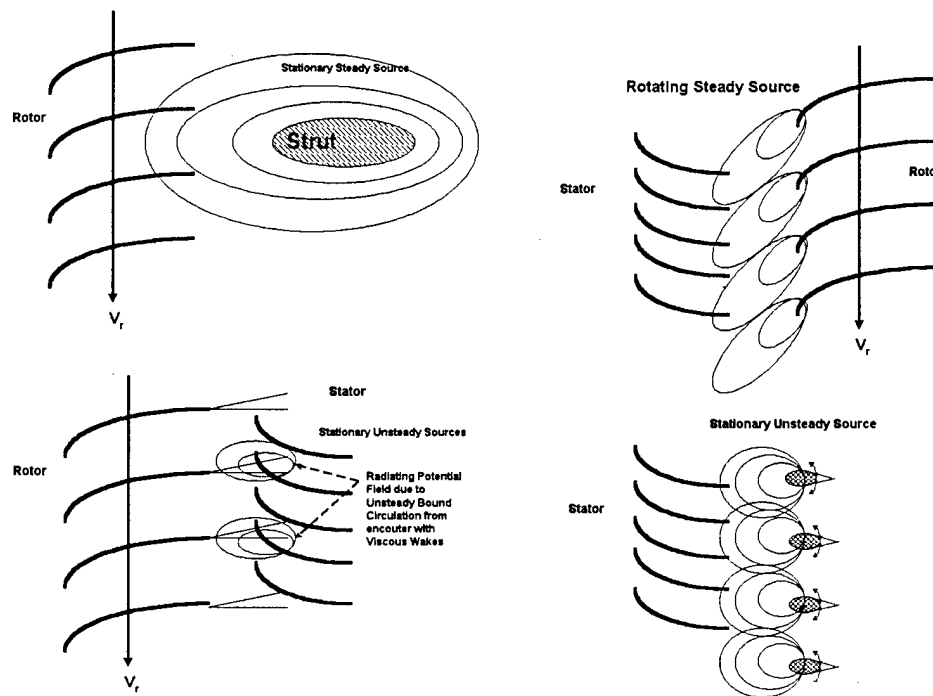


Figure 1. Classes of Potential Disturbances that can interact with upstream engine components: *Upper Left* – Stationary Steady Source; *Lower Left* – Stationary Unsteady Source due to Rotor Wake Passage; *Upper Right* – Steady Rotating Source; *Lower Right* – Stationary Unsteady Source created by Alternating Bound Circulation (in this case oscillating airfoils).

The figure at the lower left of Figure 1 represents a similar problem; however, because of the close vane-to-vane spacing of the stators, the steady potential field is generally considered to present a negligible flow distortion to the rotor. (Although this presumption is by now common knowledge, the reader may be interested in reviewing the cascade results of Sekularac [Ref. 4] that show that the higher the solidity the less flow distortion is presented by any single vane and the lower the spatial extent of these distortions from the leading- and trailing-edge planes of the vane row.) These stators experience a vortical gust with the passage of each rotor wake, which, in turn, generate unsteady bound circulation on the stators. In this case, this unsteadiness in the bound circulation creates potential disturbances that originate from stationary but unsteady sources (in the fixed frame); in this case, it should be noted that any interactions with the rotor

interact with blades in a moving (non-stationary) frame. Because the potential field is unsteady, in a compressible flow, the potential disturbances radiate (propagate) at acoustic speed, into the moving fluid. Experimental evidence that such waves are present, albeit relatively small, radiating forward from the stators in a flow behind the fan rotor in an F109 engine, is documented in Reference 5. The figure in the upper right of Figure 1 represents still another type of potential disturbance. In this case, we can think of the potential fields distorting the flow around the rotors as being steady in the rotating frame; however, to an upstream stator vane, the distorted fields are unsteady potential disturbances. This case has been documented in Reference 6. In that reference it was shown that in an incompressible flow the unsteady disturbance actually appears to propagate in the *flow direction* (i.e., the disturbance appears to move downstream) into the fan when the disturbance is measured in the fixed frame. This can be visualized by noting the canting of the potential field along the velocity triangle as suggested in the upper right of Figure 1. If a series of measurement positions in the streamwise direction upstream of the rotor are envisioned as the rotor moves downward on the page, the measurement locations farthest from the rotor will sense the arrival of a particular blade ahead of measurement locations closer to the rotor. If the flow is compressible and the rotor speed is sufficiently large, the fact that the blade is in a particular location is not communicated to the measurement location until a delay time dictated by the time associated with a signal propagating into the oncoming flow at the speed of sound. At some sufficiently-high rotor speed, the signal begins to lag behind the rotor's location, and the potential disturbance appears to radiate upstream. This too is documented for the F109 study [Ref. 6]. It is also interesting to note that, initially, the size of the disturbance measured in the F109 study was considered to be surprisingly large based on the decay predicted by incompressible analyses; however, two facts, well known in cascade analysis, should have forewarned us of the large magnitude of the potential-field disturbance. First, in compressible flows, the incompressible disturbances predicted by incompressible analyses become amplified by the Prandtl-Glauert factor. Second, although the blade-passage frequencies are high (reduced frequencies above 5), the only spatial harmonic between the rotor blades that is of interest is the fundamental. In fact, the measured disturbances ahead of the F109 fan are consistent with theoretical predictions; this consistency is documented in a Notre Dame report [Ref. 4], part of which is reported in Reference 7. This kind of radiating (upstream-propagating), unsteady potential field we define as a "*rotating*" potential source.

The fourth kind of potential source is shown in the lower right of Figure 1. In this case the source of the unsteady potential disturbance is an unsteady bound circulation at a fixed (stationary) location. This kind of potential disturbance we classify as an *unsteady stationary source*, and in some respects is similar to the case in the lower left of Figure 1; however, in this case the vanes are shown fixed in the same frame as the stationary sources. This situation is, in the absence of other obscuring disturbances, only possible in a cascade facility, such as the one that was the focus of the present grant; however, a similar disturbance was found to be created by the fan rotor blades cutting through the wake of a single IGV ahead of the fan in an F109 engine [Ref. 8]. In the F109 case, the overlaying of rotating-source responses obscured the effect of this type of source. Work investigating these stationary, unsteady-source disturbances for compressible flow in a cascade has only been performed at Notre Dame; our first investigation is documented in [Refs. 9,10]

Why Study Potential Disturbances in the Notre Dame Cascade. It may initially seem that Notre Dame's efforts to date, involving detailed unsteady disturbance and

response studies in an actual running F109 engine, have moved beyond the cascade studies carried out in the mid 1990's [Refs. 9, 10] that gave rise to a clearer understanding of upstream-propagating, potential-disturbance interactions and their importance in creating, not only large unsteady response, but in loading the trailing-edge region of the components; however, it was precisely the clean and unambiguous nature of the cascade data that allowed us to recognize what was happening in the F109 engine in the first place (see *Appendix A* for an account of the earlier cascade studies). In the preceding subsection, it was pointed out that in a cascade it is possible to create pure unsteady stationary disturbances that interact with fixed (stationary) vanes, as in the lower right of Figure 1. The importance of the F109 engine studies [Refs. 6,8,11] is that they proved that trailing-edge interactions with upstream-propagating potential disturbances do create large, trailing-edge-biased response; in fact, these F109 studies pointed out the alarming magnitude of the vane's response. In addition, the F109 studies demonstrated the fact that in the engine environment the potential disturbances are due to combinations of rotating and unsteady stationary sources like those in the upper right and lower left of Figure 1, combined [see Ref. 8, in particular]. As important as these F109 studies have been, because of this combining of disturbances from more than one source, attempts to understand the physics (mechanisms at work) of the trailing-edge interaction itself become obscured. In the F109 studies only one specially-designed and instrumented IGV was used and this allowed for a relatively simple interpretation of the rotating-source disturbance, even though this was partially obscured by the stationary-source disturbance; it is blatantly clear that if even this simple configuration complicates our understanding of the phenomena, a full-vaned IGV configuration would make understanding the trailing-edge interaction even more intractable. If the goal is to collect clean, unambiguous disturbance and trailing-edge response data from which the physics of the trailing-edge interaction might be sorted out, a return to the simple configuration in the lower right of Figure 1 is clearly indicated.

II. THE TRAILING-EDGE INTERACTION

The most important finding of the mid-1990 cascade studies was the large trailing-edge response. This unsteady trailing-edge loading is also, by far the most unexpected result of the Notre Dame findings. The character of the response elicited by upstream-propagating potential disturbances interacting with a sharp-trailing-edge vane is best described by examining the mid-1990 Notre Dame cascade results [Refs. 9,10, and see Figure A10 in *Appendix A*). Although limited to measurements back to 80% chord, the distinct character of the cascade response is a large unsteady pressure difference near the trailing edge, decaying with increasing distance from the trailing edge (i.e., toward the leading edge); the unsteady pressure difference appears to go to zero at the leading edge. It might be noted by the reader that if this response were reversed (i.e., large response at the leading edge and decaying toward the trailing edge) it would seem quite similar to classical leading-edge response for a thin airfoil. As is well understood, the large response at the leading edge is due to a mathematical dilemma, which was solved by the allowance of a leading-edge singularity, and the decay toward the trailing edge is due to the disallowing of a trailing-edge singularity (i.e., the Kutta condition). Crighton, and Leppington found a similar mathematical dilemma when examining the trailing-edge

response of a thin flat splitter plate dividing a shear flow when exposed to upstream-propagating acoustic disturbances [Ref. 12]; they *chose* to disallow the trailing-edge singularity (i.e., they chose to take a strict interpretation of the Kutta condition, “*full Kutta Condition*”). Their theoretical *choice* that no unsteady pressure singularity occurred at the plate’s trailing edge led to the mathematical requirement that the flow in the shear layer leaving the trailing edge be directed at time-varying angles to the direction parallel to the plate. Subsequent experiments admitting acoustic waves tuned to the most-unstable Helmholtz instability of the shear layer, demonstrated an enhanced growth in the shear layer and led to subsequent development of the trailing-edge receptivity problem. These subsequent experimental results also led to widespread acceptance of Crighton and Leppington’s *choice* of imposing the “full Kutta condition” on the outer solution of the unsteady-shear-layer and trailing-edge problem as the only proper trailing-edge condition.

In fact, we are not the first to have questioned this strict interpretation of the Kutta condition. Experimental results by Gallus et. al. [Ref. 13] showed a relatively-large unsteady loading toward the trailing edge of stators placed upstream of a rotor and lead them to question the unsteady Kutta condition. Dring et. al. [Ref. 14] also found relatively-large, trailing-edge unsteady pressure differences near the trailing edge of upstream stators in front of a rotor, again questioning the Kutta condition. Few computational studies have concluded that unsteady trailing-edge loading is a problem, probably because most are theoretically based and disallow trailing-edge singularities; however, a study by Lewis et. al. [Ref. 15] used an unsteady Euler code to investigate the interaction between an upstream vane and a downstream rotor. No Kutta condition was imposed; rather, they depended on numerical viscosity to cause the flow to separate at the trailing edges. Their computations very clearly show unsteady loading on the stator which is biased toward the trailing edge and has a finite unsteady pressure difference at the trailing edge. It should be pointed out that in none of the above cited references was the magnitude of the unsteady pressure differences at the trailing edges as large as those measured in the Notre Dame F109 studies; however, they were, in some cases, on the same order as the pressure differences measured in the Notre Dame cascade. It should also be noted that the experiments cited here [Refs. 13,14] were in rotating rigs, which, as we have shown in Reference 8, must have had a mixture of rotating and stationary sources.

Thus, we are forced to conclude that there is now an increasing body of data, both by us and by others, showing that upstream-propagating potential disturbances not only elicit large unsteady response on upstream components, but also appear to elicit a trailing-edge singularity. It may, in fact, be this trailing-edge amplification of response to otherwise perturbation disturbances that causes such large unsteady response at relatively-large distances from the sources. This being the case, it seems unquestionable that the physics of this trailing-edge response be properly understood, once and for all. It was to this end that we attempted to prepare and run the “*perfect*” experiment. Based on the types of disturbances described above, a return to the unsteady, compressible cascade made and continues to make perfect sense. In this context, the collection of response data must also be accompanied by the cleanest possible potential-disturbance source. In the earlier studies [Refs. 9,10], we felt we had discovered such a source, *von Karman shedding from circular cylinders*.

III. USE OF VON KARMAN VORTEX SHEDDING FROM CIRCULAR CYLINDERS FOR UNSTEADY DISTURBANCE SOURCES

In the earlier cascade studies the potential disturbance source was a row of circular cylinders placed at mid passage, 0.8 vane chords downstream of the vane-row trailing edges (see Figure A1 in *Appendix A*). As described in References 9 and 10, although we had expected to have to use active control to have all the cylinders shed in phase, for whatever reason, the rods shed in phase without the need for active control. The character of the potential source(s) can be envisioned as shown in Figure 2.

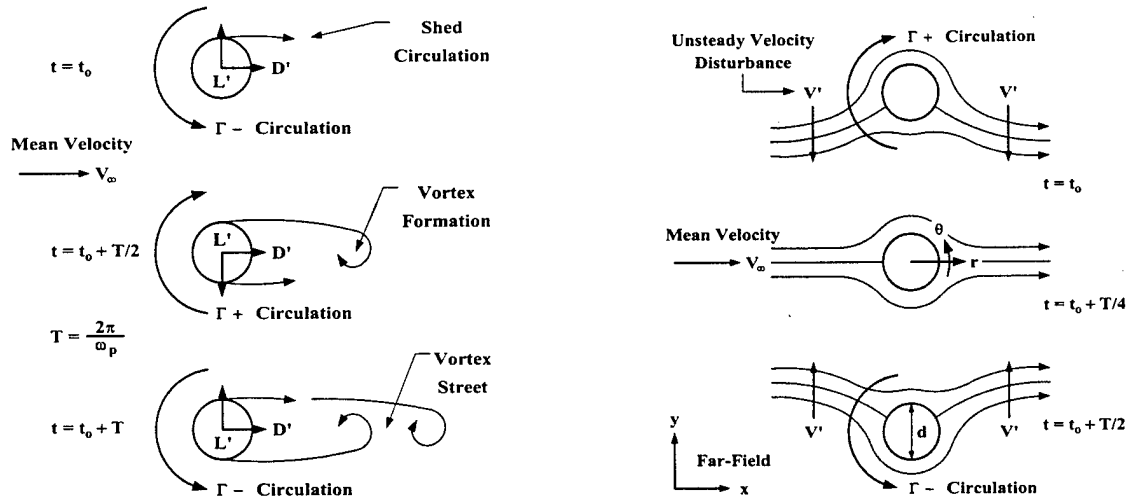


Figure 2. Von Karman Shedding from a Single Rod

During one cycle of lift there are two cycles of drag. As described in the *Appendix A*, for a vane upstream of a row of these rods, all shedding in phase, the vane surfaces will experience a cycle of forcing normal to the surface for one cycle of lift at the primary (fundamental) frequency. During this lift cycle, the surface sees two cycles of surface-parallel forcing, at the first harmonic. This combination of normal forcing and surface-parallel forcing proved instructive in the sense that disassembling the response signal into its fundamental and harmonic content allowed us to show that only the surface-normal component gave rise to an apparent trailing-edge singularity, while the surface-parallel disturbance response appeared to go to zero at the trailing edge. In addition, the phase of the surface-parallel response was in phase and therefore gave no unsteady pressure difference, while the surface-normal response was out of phase across the vane so that the pressure difference had larger magnitude than either the upper or lower response alone. Because the rods worked so well in the earlier studies, it is natural that we chose the same method of forcing for the present studies.

Before leaving this section, it should be noted that after we ran into problems keeping the shedding in phase (which will be addressed in a later section), we considered alternative mechanical methods of providing an oscillating bound circulation. The method shown schematically in the lower right of Figure 1 was considered; however, the oscillation frequency of approximately 7 kHz made such a system impossible to build. Other methods we considered included looking at alternating *Magnus Flaps*; even when

we came up with a design that could produce four oscillations per rotation of a slotted manifold, Magnus Flaps would have required rotating a manifold at 52,000 RPM. Again, Magnus Flaps presented another impossible design. In the end, we concluded that any forcing to produce the potential disturbances had to incorporate von Karman shedding in some form, which might include forcing the multiple rod in order to phase lock the shedding.

IV. OVERCOMING THE SHORTCOMINGS OF THE EARLIER STUDY

The work of the present research returned to a cascade environment to reexamine the results of the earlier studies, but attempted to overcome the shortcomings of the earlier studies. With the choice of the rods as the potential disturbance sources, the main objective of the present work was to collect data farther back on the airfoil (i.e., beyond the 80% chord location of the earlier studies) as well as document the potential-disturbance velocity field *with* and *without* the responding blades present in the cascade. The objective of documenting the velocity field both *with* and *without* the vane row required that the cascade be unloaded. Having an unloaded cascade also seemed to make sense in terms of the resolution of the unsteady forced response. Assuming that the forcing from the downstream row of rods all shedding in phase, the forcing would be independent of the side of the vane that was responding, except the phase on the surface normal forcing should be π out of phase with the opposite side. Additionally, it seemed logical to start with a single vane, centered on the test section with two half vanes at the walls. To accommodate the placement of transducers near the trailing edge, we chose a relatively thick airfoil and an airfoil section that maintained its thickness toward the trailing edge. Since the same vane design was planned for the instrumented IGV in the ongoing F109 engine studies, the first test was using oil visualization to see if the airfoil's flow remained attached in steady and unsteady flow; it stayed attached. With these considerations in mind, the new test section is shown schematically in Figure 3.

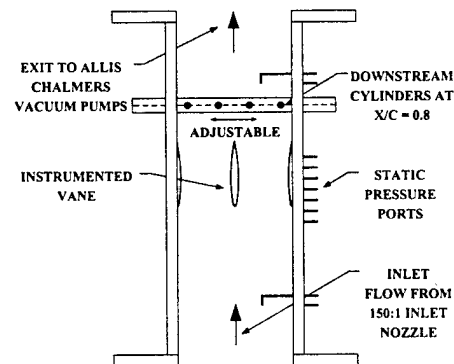


Figure 3. New Cascade that Accommodates Pressure Transducers back to 93% Chord

Experimental Parameters. The new, unloaded cascade, shown schematically in Figure 3, formed the test section of one of Notre Dame's in-draft transonic tunnels; the cross-section was 3.85 in. \times 3.95 in. The new cascade used NACA 16-0012 airfoils for the vanes; in the initial configuration a single vane was instrumented with eight, surface-

mounted ultra-miniature transducers located along the mid-span region from $x/c = 0.54$ to 0.93. Two half vanes were mounted on the walls of the test section. It should be noted that having a single instrumented vane overcame another shortcoming of the earlier studies. In the earlier studies that used production-hardware stator vanes from the F109 engine, the vanes were so thin that not only did they allow for the farthest aft measurement location to be at 0.8 chord, only two instrument locations were possible on any single vane. This meant that the cascade had to be reconfigured eight times to obtain a single nominal vane response.

As mentioned above, the unsteady forcing was again established through von Karman vortex shedding from a row of cylinders placed 0.80 vane chords downstream, where the cylinders were aligned parallel to the vane span. Once again no active shedding control was used; however, the character of the shedding was monitored via surface-mounted transducers on the cylinders. Two-hundred data sets were collected at each transducer for four free-stream tunnel Mach numbers, M_∞ , ranging from 0.33 to 0.51, two reduced frequencies, k , of 5.6 and 7.5, and two forcing configurations (four and two-cylinder forcing). The collected data were phase-locked via one of the pressure transducers embedded in the forcing cylinders.

V. EARLY RESULTS OF THE PRESENT RESEARCH

(or *DROWNING WHILE STANDING KNEE DEEP IN THE STREAM OF HAPPINESS*)

AMMi Transducer Results. Our progress in this effort was delayed by two early, in retrospect, unfortunate decisions. The first of these was that Notre Dame was teamed in this effort with the Air Force Institute of Technology (AFIT) and, early on, the effort was divided so that Notre Dame would concentrate on getting the pressure-response data and AFIT would look at the velocity field [Ref. 16]. This teaming arrangement led us to concentrate on the pressure response rather than the velocity field, which might have tipped us off to a possible problem in the in-phase shedding on the forcing rods.

The second was a decision to try using some new pressure transducers. Using these new transducers, we obtained incomplete, but what appeared to be excellent early results; these were obtained shortly after receiving the grant and led us to believe that things were going well. The new surface-mounted pressure transducers were manufactured by Advanced Micromachines Incorporated (AMMi) [see Figure 4].

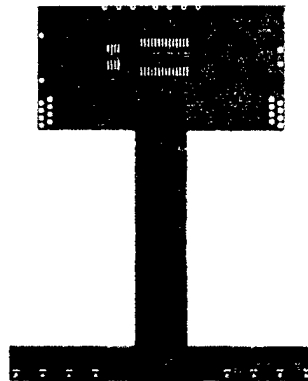


Figure 4. AMMi Surface-Mounted Miniature Pressure Transducers.

We worked with Dr. Mitch Wolff from Wright State University to check the dynamic range on these transducers and they had excellent response well beyond 50 kHz. When we applied them to the vane described in *Experimental Parameters*, we found that only 3 of the eight transducers were working. These happened to be at 0.58 chord on the upper surface, 0.58 chord on the lower surface, and 0.75 chord on the lower surface, as shown in Figure 5. Results from testing the vane with only the three operating transducers looked exactly the way we expected them to look based on the earlier loaded cascade tests of References 9 and 10. These results, run at a cascade inlet Mach number of 0.38, showed the expected trigger response (see Figure 6), and gave relatively large unsteady response as shown in Figure 7. It is also clear from Figure 7 that the signal at 0.75 chord was larger than those at the two 0.58 chord locations. The signal character looked as expected, and we were able to construct two-frequency representations of the 200-enssembled signals in the manner used in the earlier studies. Figure 8 shows one of the reconstructed signals laid over the original 200 ensemble, phase-locked data, where it is clear that the two-frequency representation did a beautiful job in reconstructing the character of the signal; the other two signals gave similar excellent results.

Location of Pressure Transducers on Vane

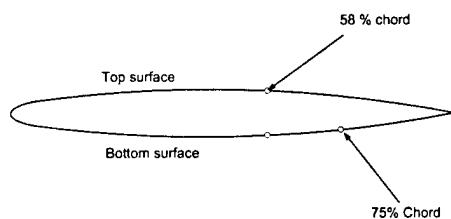


Figure 5. Schematic of Vane Showing the Location of the Three Operable Transducers.

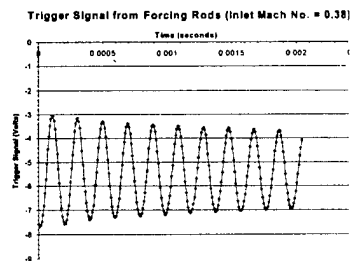


Figure 6. Two-Hundred Phase-Locked Ensemble of Trigger Signal.

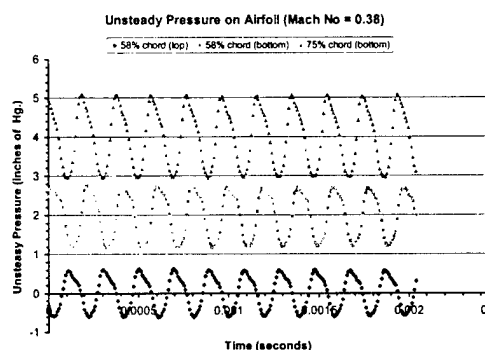


Figure 7. Two-Hundred Ensemble Phase-Locked Response at 0.58 and 0.75 chord.

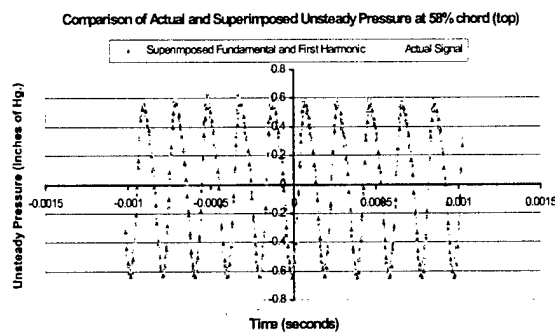


Figure 8. Two-Frequency Reconstruction Overlaid onto the Ensemble at 0.58 chord.

Figures 9 shows the fundamental and harmonic portions of the two-frequency-reconstructed data from the upper and lower 0.58 locations laid over each other.

Figure 9, in particular appeared to reinforce the correctness of our decision to use only one, uncambered vane in the following sense. First, note that the upper and lower fundamental-frequency responses were nearly identical, but are 180° out of phase. Second, note that the two harmonic signals are nearly identical and in phase. These were exactly as we expected them to be (refer to the discussion of the forcing expected from the downstream rods, where the normal component shifts from being downward to upward once per cycle, the pressure response acting first toward the surface on the upper and away on the lower, then away on the upper and toward on the lower). At the same time, the surface-parallel disturbance should be at twice the fundamental frequency and be identical on both the upper and lower surface. Figure 10 also reinforced our sense that all was well; Figure 10 shows that the phase relationship of the two locations, both for the fundamental and the harmonic, were consistent with an upstream-traveling wave having its origin downstream of the vane's trailing edge; the same propagation model used in the earlier study, worked well on these results. Even the difference in amplitude between the upper and lower surfaces for the fundamental-frequency portion of the signals at the 0.58 chord location (see Figure 9) appeared to be explainable by the fact that the vane was slightly misaligned in the tunnel.

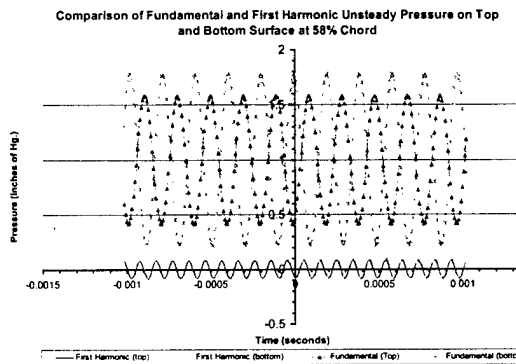


Figure 9. Upper- and Lower-Surface Fundamental and Harmonic Signals.

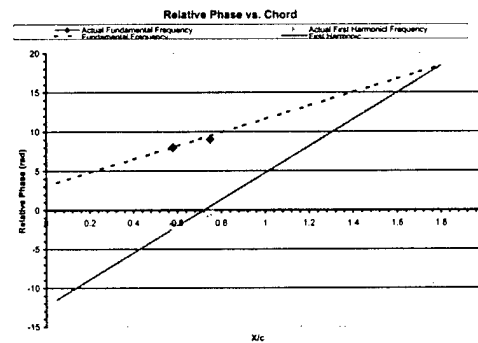


Figure 10. Phase Maps for the Fundamental and Harmonic Signals.

Kulite Transducer Results. Based on the excellent quality of the data, the apparent applicability of the AMMi transducers and our determination that the problem with the transducers was that the tiny leads had lost continuity, we lost more time in negotiating with AMMi to produce a new set of corrected transducers. When they arrived 3 months later, we found that, at best, only 4 of the eight transducers operated. This led to our decision to go to Kulite transducers, like those used in the earlier studies. Figure 11 shows the locations of the transducers on the vane. Once the new, instrumented vane was completed, we returned to testing under the assumption that everything was on track. Figure 12 shows a representative selection of RMS unsteady pressure versus chord location for a set of runs for Mach numbers from 0.33 to 0.51, with two different diameter forcing rods. Notice that although there appears to be a rapid fall off in amplitude at the farthest aft location, the $M = 0.51$ case, in particular, appears to be following the general trend of the earlier test, also shown in the figure is the Fabian, et.

al. data; although, the increase in the amplitude toward the trailing edge is not as dramatic as in the earlier studies.

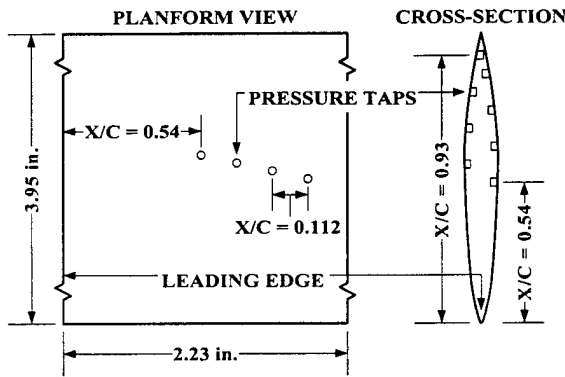


Figure 11. Transducer Locations on Vane.

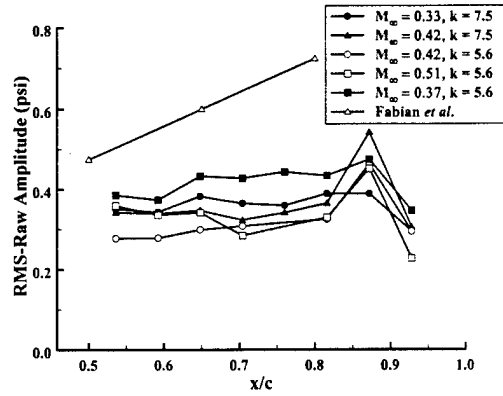


Figure 12. Raw RMS Unsteady Pressure Amplitudes vs. Chord Location

Initially, this suggested that, perhaps, the hypothesized trailing-edge singularity might not actually exist (it should be noted that large unsteady pressure differences across an IGV at 0.94 chord have now been measured in F109 engine tests, Refs. 8, 11). But, once we had disassembled the data into two-frequency representations, we began to suspect that there was something wrong with the data.

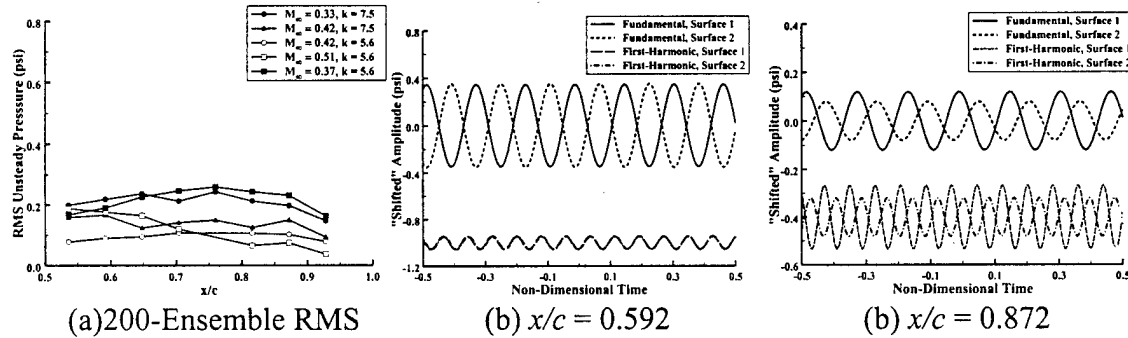


Figure 13. (a) RMS Unsteady Pressure After Ensemble Averaging; (b) Two-Frequency Amplitudes of Fundamental and Harmonic at 0.592 Chord; (c) Two-Frequency Amplitudes of Fundamental and Harmonic at 0.872 Chord.

The first indications of a problem appeared after examining the 200-ensemble, phase-locked data for various run conditions, as shown in Figure 13; notice that for $M = 0.51$, the trend seen in the raw RMS data is reversed. Secondly, while the two-frequency amplitudes at 0.592 chord, Figure 13(b), look similar to the three-transducer AMMi set of Figure 9, the relationships referred to for Figure 9, are jumbled up in Figure 13 (c) at the 0.872 chord location. In fact, what we found in these data was that a two-frequency model did a very poor job of representing the data at measurement locations aft of 0.75 chord; for these aft locations, as many as four harmonics were required to begin to capture the structure of the 200-ensemble. Setting aside these problems for the moment,

as in the earlier studies, we began to look at the trends in the amplitudes of the fundamental component and its harmonic as a function of chord position.

Fundamental Amplitude. The amplitudes of the fundamental portion of a two-frequency representation of the unsteady pressure response on the vane as a function of chord location, for a range of test conditions, are shown in Figure 14. First, no increase in amplitude occurs beyond $x/c \approx 0.75$; this may be compared with the earlier results; a representative set of data for Mach 0.43 is shown in Figure 15 [Ref. 9,10].

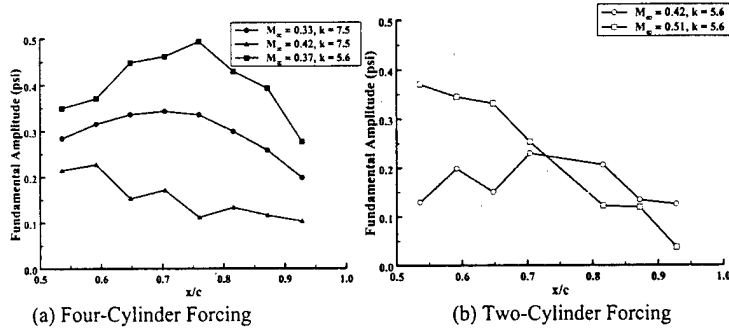


Figure 14: Fundamental Amplitudes: Four-Cylinder and Two-Cylinder Forcing.

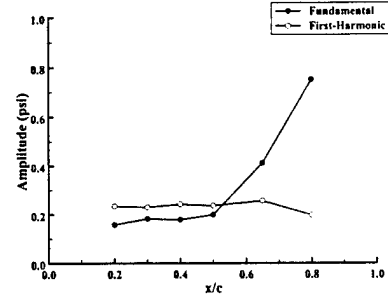


Figure 15: Unsteady Pressure Amplitudes for the Fundamental and Harmonic at $M_\infty = 0.43$.

Figure 15 shows the amplitudes of two-frequency-decompositions for both the fundamental and harmonic portions of the decomposition. Notice that in the earlier studies, the unsteady pressure amplitudes of the fundamental component (i.e., that portion of the response due to forcing normal to the surface) not only increased sharply toward the final measurement location at 0.8 chord, but the amplitudes are much larger than in the present data, reaching peak-to-peak amplitudes of greater than 1.0 psi (approximately 50% of the tunnel static pressure). On the other hand, the amplitudes in the current investigation are, in some cases, larger in amplitude than the earlier studies at 0.5 chord.

Normalized First-Harmonic Amplitude. It might be noted in Figure 15 that the harmonic response (i.e., due to forcing parallel to the surface) in the earlier study was actually higher than the fundamental in the forward portion of the vane. A better way of comparing the harmonic to the fundamental is to normalize the magnitude of the harmonic response by the magnitude of the fundamental response at each chord location. The normalized, harmonic amplitudes for the earlier study for $M_\infty = 0.43$, $k = 4.3$ corresponding to the data in Figure 15 is shown in Figure 16(a), and similar normalized amplitudes corresponding to the two of the data sets in Figure 14(a) are shown in Figures 16 (b) and (c), for $M_\infty = 0.42$, $k = 7.5$ and $M_\infty = 0.37$, $k = 5.6$ cases, respectively. It can be noted in Figure 16(a) that the harmonic content of the signal at the forward portion of the vanes in the earlier study contains most of the energy at the forward portion of the vane and diminishes to a very small portion of the response by 0.8 chord, with a clear diminishing amplitude toward the trailing edge. On the other hand, in the present, single, unloaded vane response for the four-cylinder forcing the harmonic content is increasing toward the trailing edge. In the $M_\infty = 0.37$, $k = 5.6$ case, the harmonic content has little

variation up to the $x/c \approx 0.816$ location, increasing near the trailing edge; although, the harmonic content never exceeds the fundamental. In the $M_\infty = 0.42$, $k = 7.5$ case, the harmonic content not only exceeds the fundamental, but also exhibits a systematic increase along the vane. Moreover, comparison of the $M_\infty = 0.42$, $k = 7.5$ data in Figures 14, suggests that a continuously-increasing harmonic appears to correlate with a continuously-decreasing fundamental. Similarly, the approximately-constant, then increasing, trend of the $M_\infty = 0.37$, $k = 5.6$ harmonic content in Figure 16(b) appears to be associated with an increasing, then decreasing, fundamental content.

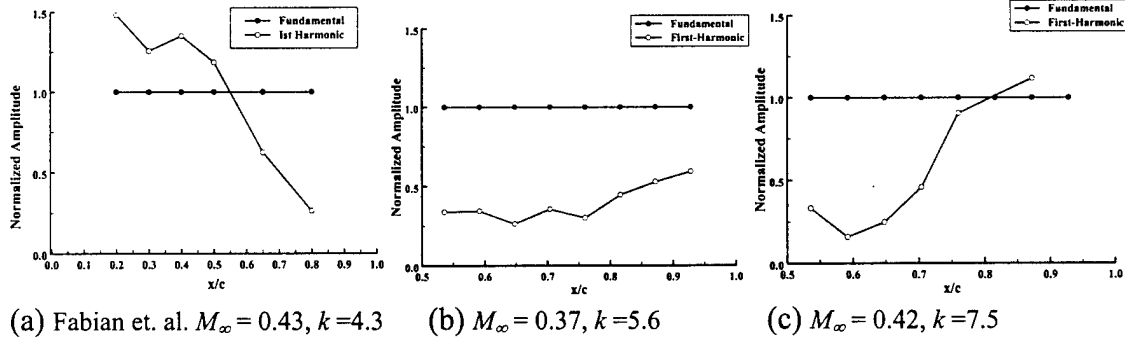


Figure 16: Normalized Amplitudes for Earlier Study and the Present Study, Four-Cylinder Forcing.

This association is also suggested in the normalized harmonic amplitudes for the two-cylinder forcing cases. As shown in Figure 17(a), the harmonic content at $M_\infty = 0.42$, $k = 5.6$ shows little change, varying only slightly near the trailing edge; comparing this behavior with the character of the fundamental content shown in Figure 14(b), shows that the nearly-constant harmonic amplitude region correlates with a nearly constant fundamental response, and the increase in the harmonic again correlates to the decrease in the fundamental content in the response. Similar comparisons for the $M_\infty = 0.51$, $k = 5.6$ case show a harmonic content increase along the chord to be associated with a decrease in the fundamental content. In the Fabian *et al.* case the normalized first-harmonic content [Figures 15 and 16 (a)] decreases continuously over the vane, correlating to a continuous increase in the fundamental content.

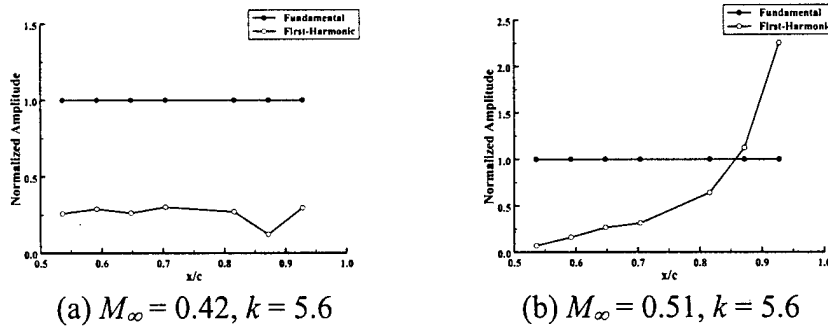


Figure 17: Normalized Amplitudes for Two-Cylinder Forcing.

It should also be noted that a decrease in the fundamental content in the response and increase in the harmonic content in the present study also correlated in a rise in the amplitude of additional harmonics needed to decrease the error in the harmonic reconstruction of the 200-ensemble unsteady pressure response. This correlation between the rise in the number of harmonics needed to more-faithfully reproduce the character of the response is a reflection of the fact that the response contains much more structure toward the trailing edge than near the midchord. Coupled with the fact that the ensembles decrease the RMS amplitude of the response, as noted earlier, and the fact that the earlier studies retained their faithful reproduction of the response signal with only a two-frequency representation, led us to believe that we had a problem with a well-behaved, in-phase shedding on our forcing cylinders in the present study.

Cylinder Vortex Shedding. Unlike the results of earlier studies, once we investigated the shedding behavior of the cylinders, we were disappointed to find that the relative phase of the vortex-shedding across the row of forcing cylinders depended heavily upon M_∞ , k , and configuration. Moreover, the shedding relative phase was found to play an essential role in the vane pressure response. For example, out-of-phase shedding produced anomalous pressure-response results, while in-phase shedding produced data more comparable, in some ways, to that of the earlier studies.

The character of the trigger signals also differed from that of earlier studies. In the earlier studies, the trigger signals showed no signs of higher-harmonic content (i.e., the trigger signals were nearly pure sinusoids at the fundamental frequency), while the current trigger data exhibited significant harmonic content under most conditions. Figure 18 shows representative trigger signals from the current investigation. Note that under certain flow conditions the signals show significant harmonic content, while at other conditions they do not. The effect of this harmonic content, in terms of vane pressure response, is unclear at this time; however, we consider the higher-harmonic content to be undesirable.

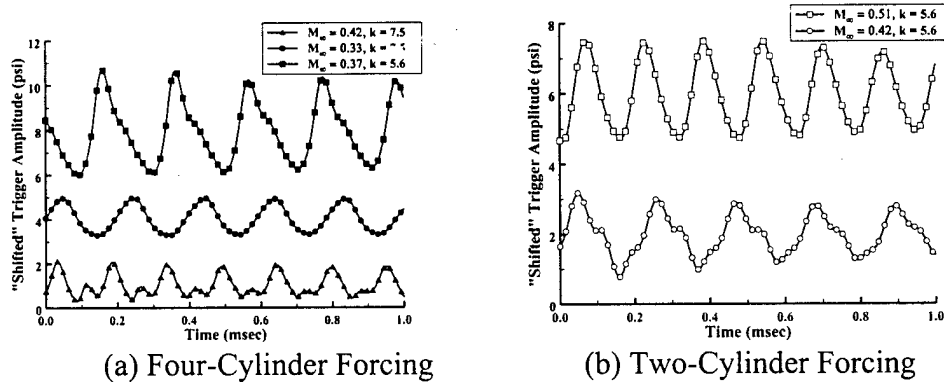


Figure 18: Vertically-Shifted Trigger Signals: Four-Cylinder and Two-Cylinder Forcing.

In addition to the structure in the trigger signal, the relative phase of the shedding between cylinders appears to be crucial to the harmonic content in the response signal near the aft portion of the vane. Since the entire objective depends on the quality of the potential disturbances, we view this complication in our work to be a showstopper. For

this reason, the emphasis of the work shifted toward the production of in-phase shedding of the forcing rods.

VI. IN SEARCH OF THE PERFECT POTENTIAL DISTURBANCE (or the Creation of In-Phase Forcing-Cylinder Shedding).

As discussed in an earlier section of this report, it is essentially impossible to produce a 7 kHz signal using mechanical devices. It still appears that forcing using von-Karman shedding from circular cylinders aligned parallel to the span of vanes and placed downstream of the vanes provides very clean and interpretable response if they can be made to shed in phase. To us, if we are able to make the rods shed in phase, these rods provide a perfect method to produce upstream-propagating potential disturbances. To this end, we returned to the earlier configuration to assure ourselves that the rods were shedding as we had presumed they were in the earlier studies, and, indeed, they were. Although we are not reporting the work here, we have now collected phase-locked velocity data in the old cascade configuration (i.e., configuration shown in Figure A1 of the *Appendix A*); suffice to say, because of the presence of the vane wakes, these data are difficult to interpret without the benefit of the velocity field in the absence of the vanes, as was done in the F109 studies. The problem is that with the loaded vanes absent, the flow separates from the wall of the turned duct; further, in a straight duct with the same rod geometry, i.e., same spacing and alignment angle to the tunnel axis, still the rods do not shed in phase. Having tried so many things to achieve passive locking to this point, we have no illusions about having to turn to some sort of active control mechanism to lock the shedding on all the forcing cylinders. We have already made some attempts at this control. Our first attempt at a control technique was to oscillate the cylinders in a plane normal to the cylinders span and normal to the oncoming flow. To date we have tried speaker coils; however, at the frequencies required (5KHz to 9KHz) the displacements achievable using the coils has not been able to phase-lock the rods' shedding. As mentioned earlier, a number of mechanical designs have been considered, including mechanical cam arrangements; however, these would require shaft rotations of from 50,000 to 200,000 RPM and we consider these impossible.

We are now trying to use plasma actuators [Refs. 17,18]; the equipment to drive these actuators has already been procured. Similar actuators have been used to control flows with Mach numbers as high as 3.5, so we have high expectations for this control solution. A number of preliminary plasma-actuator experiments have been carried out in the last six months of the Grant, in cooperation with the Air Force Academy, to study the specific ability of the plasma actuators to lock von Karman vortex shedding. At this writing, a lower-frequency experiment with two, 1.5-inch cylinders spanning one of Notre Dame's low-speed wind tunnels is being planned. We are in the process of applying 3/8-inch electrodes along the full span of the rods, symmetric to the centerline of the circular cross section on the downstream side of the cylinders (see Figure 19). A 1-1/2 inch layer of 2-mil Teflon tape will be applied over the electrodes, and a 1-1/2 inch layer of 2-mil Kapton tape on top of the Teflon. Two 3/8-inch electrodes will then be applied on top of the two layers of insulation at the two upstream edges of the first electrodes. We know from tests that we have made with this electrode configuration that

the plasma will form at the downstream edge of the upper electrodes, and when the plasma is switched on, it produces a downstream jetting of the air. We plan to turn the plasma on and off at the beat frequency between the excitation frequencies of the two lower electrodes and the two upper electrodes.

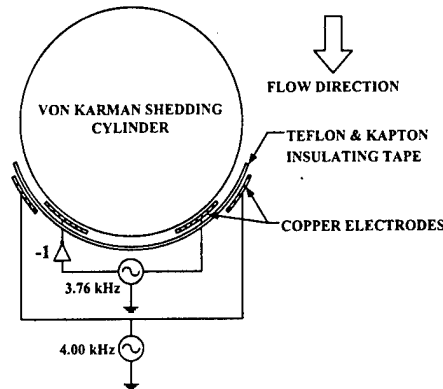


Figure 19. Plasma-actuator excitation scheme for the 50-ft/s experiments

We plan to excite the upper electrodes at 4 KHz at $\pm 5,000$ volts. The lower electrodes will be excited at varying frequencies to produce a beat frequency at the appropriate von Karman shedding frequency; for a tunnel velocity of 50 ft/s the beat frequency will be approximately 240 Hz, thus the inner electrodes will be driven at 3760 Hz. These two electrodes will be excited 180° out of phase by exciting them both with the same signal, but one of the outputs will be passed through an inverting amplifier. Two amplified signals, one at 4000 Hz and the other at a variable frequency will be produced using identical set ups; these will be made up of a square wave from an HP 3312A function generator fed to a Crown CE 1000 audio amplifier and its ± 36.5 Volt signal passed through a Corona Magnetics CMI-5012-0040, 1:137 transformer, the output of which being the excitation signal for the electrodes.

We have already tested the electronics and electrode configuration on a single-rod experiment in a tunnel at the Air Force Academy; while the shedding appeared to be consistently associated with the shedding on the cylinder when the actuator frequency was fine tuned to the shedding frequency, the single-rod experiments are inconclusive as to whether the plasma actuators will be able to phase lock the shedding on multiple cylinders. The success of the actuators being able to phase lock multiple cylinders should be known once the Notre Dame experiments are complete.

Assuming that the plasma actuators are successful in producing controlled shedding on the two-cylinder, 1-inch rod experiments, we plan to test the actuators at the higher frequencies in the Notre Dame cascade. Since flow visualization is impractical at the high frequencies we will produce in the cascade, imbedded Kulite pressure transducers, whose tap hole is oriented at 90° to the oncoming flow, will be mounted in the $\frac{1}{4}$ -inch excitation rods. The use of $\frac{1}{4}$ -inch rods will, in fact, create reduced frequencies on our present unloaded, single-vane cascade configuration that will be nearly identical to the earlier loaded-cascade reduced frequencies.

VII. DISCUSSION AND CONCLUSIONS

At this writing, the potential-disturbance studies in the F109 turbofan engine continue under separate funding, but this effort, for now, has lost continued funding. As best I can read the rationale for the loss of funding, it is because of the unexpected complications that we experienced in producing clean, in-phase shedding from the forcing rods. It is distressing to me that the evaluation of this basic research effort depends on the fact that there is risk involved in the possibility that we will fail to produce clean potential disturbances. We may indeed fail; however, the alternative is that the interaction between a sharp trailing edge and upstream-propagating potential disturbances cannot be sorted out in other types of rigs that are presently being used, including our own F109 studies. The reason is the ambiguity introduced by not-well-behaved upstream-propagating disturbances. The results from the F109 studies, as well as the results reported here for the cascade, are evidence of this fact. The potential for developing data that will be able to sort out this, now-proven first-order disturbance in turbine engines, is so crucial that it seems to me that just the investigation into producing the perfect potential disturbance is worth the cost of a basic-research grant. It is for this reason that I complete this reporting with a great deal of uneasiness. For this reason, although our funding has ended, I will not give up on pursuing the problem.

Toward the end of this grant, we were encourage to return to a loaded cascade arrangement and attempt to document the unsteady velocity field between the vane trailing edges and the forcing rod. As was mentioned in the body of this report, we did this; however, it became clear that knowledge of the potential disturbance both *with* and *without* the vanes present is essential to properly understand the interaction. This, more than any other single set of results, convinced me that we must return to our quest for producing phase-locked shedding on the rods.

Acknowledgement/Disclaimer

The Air Force Office of Scientific Research, USAF, sponsored this work under grant/contract number F49620-99-1-0251. The views and conclusions contained herein are those of the author and should not be interpreted as necessarily representing the official policies or endorsements, either expressed or implied, of the Air Force Office of Scientific Research or the U.S. Government.

References

1. Thompson, D., "The National High Cycle Fatigue (HCF) Program," *Proceedings of the 3rd National Turbine Engine High Cycle Fatigue Conference*, February 1998.
2. Kemp, N.H. and Sears, W.R., "Aerodynamic Interference Between Moving Blade Rows," *J. Aeronautical Sciences*, **20** (9), Sept 1953, pp. 585-597.
3. Ng, W.F., O'Brien, W.F. and Olsen, T.L., "Experimental Investigation of Unsteady Fan Flow Interaction with Downstream Struts," *Journal of Propulsion and Power*, **3** (2), March-April, 1987, pp. 157-163.

4. Sekularac, A, *Potential-Field Disturbances in a Loaded Cascade of Airfoils*, M.S. Thesis, University of Notre Dame, July 2000.
5. Falk, E. A., Jumper, E. J., and Haven, B. A., "Upstream-Propagating Potential Waves Elicited from the Stator Row Downstream of a Fan," AIAA Paper 99-2805, June, 1999.
6. Falk, E.A., Jumper, E.J., Fabian, M.K. and Stermer, J., "Upstream-Propagating Potential Disturbances in the F109 Turbofan Engine Inlet Flow," *Journal of Propulsion and Power*, **17** (2), March-April 2001, pp. 262-269.
7. Sekularac, A., Falk, E.A. and Jumper, E.J., "A Conformal Mapping Analysis of Cascade Trailing-Edge Flows," AIAA Paper 2000-0229, January 2000.
8. Kirk, J.F., Falk, E.A., Jumper, E. J. and Haven, B.A., "Unsteady Forcing of an IGV Forward of a Fan in Subsonic Flow: Phase Results," AIAA Paper 2001-3474, July, 2001.
9. Fabian, M.K., Falk, E.A. and Jumper, E.J., "Upstream-Propagating Potential Disturbances Interacting with a Compressible Cascade," *Journal of Propulsion and Power*, **17** (2), March-April 2001, pp. 240-247.
10. Fabian, M.K. and Jumper, E.J., "Rearward Forcing of an Unsteady Compressible Cascade," *Journal of Propulsion and Power*, **15** (1): 23-30, 1999.
11. Falk, E.A., Kirk, J.F., Jumper E.J., and Haven, B.A., "Unsteady Forcing of an IGV Forward of a Fan in Subsonic Flow: Amplitude Results," AIAA Paper 2001-3475, July, 2001.
12. Crighton, D.G. and Leppington, F.G., "Radiation Properties of the Semi-Infinite Vortex Sheet: the Initial-Value Problem," *Journal of Fluid Mechanics*, **64**, part 2, 1974, pp. 393-414.
13. Gallus, H.E., Lambertz, J. and Wallmann, T., "Blade-Row Interaction in an Axial-Flow Subsonic Compressor Stage," *Journal of Engineering for Power*, **102** (1), 1980, pp. 169-176.
14. Dring, R.P., Joslyn, H.D., Hardin, L.W. and Wagner, J.H., "Turbine Rotor-Stator Interaction," *Journal for Engineering for Power*, **104**, (4), 1982. pp. 729-742.
15. Lewis, J.P., Delaney, R.A. and Hall, K.C., "Numerical Prediction of Turbine Vane-Blade Aerodynamic Interaction," *Journal of Turbomachinery*, **111**, 1989, pp. 387-393.

16. Wade, P.C., P. I. King, D. R. Hopper, E. J. Jumper and A. Asghar, "Velocity Fields Upstream of Rods Used for Forcing Unsteady Compressible Cascades," AIAA Paper 00-3229, July 2000.
17. Roth, J.R. and Sherman, D.M., "Boundary layer Flow Control with a one Atmosphere Uniform Glow Discharge Surface Plasma," AIAA Paper 98-0328, Jan 1998.
18. Corke, T.C. and Matlis, E., "Phased Plasma Arrays for Unsteady Flow Control," AIAA Paper 2000-2323, Jun 2000.

Appendix A: Mid-1990 Notre Dame Cascade Results

Notre Dame Unsteady, Compressible Cascade. The Notre Dame cascade forms the test section of a transonic in-draft tunnel located in the Hessert Center for Aerospace Research. The tunnel is driven by three 3,310-cubic-feet-per-minute, Allis-Chalmers vacuum pumps, which may all or selectively be used to drive the tunnel. A schematic of a top view of the cascade-section geometry in the configuration at the time of the mid 1990's experiments is shown in Figure A1. For the testing described in this Appendix, the turning vanes were production-hardware, stator vanes from the single, axial-flow, compression stage of a Honeywell F109 turbofan engine; although the vanes have a varying chord from tip to hub, the chord variation is slight and they have no twist. The nominal chord of the vanes is 1.28 inches and the blade spacing was 0.84 inches. The 42.5° cascade turning angle of the flow represents an average value when compared to the design 39.8° and 45.2° turning of the stator tip and hub, respectively, of the actual F109 engine. In the engine, the stators are swept aft from the hub to tip; however, in the cascade the vanes were mounted vertically to form a nominal two-dimensional linear cascade. The cross-sectional inlet and outlet of the cascade are 4 in X 4 in. Four midstream vanes and two wall vanes form five flow passages. A variety of tests were run verifying that the flow was two dimensional over the instrumented region of the vanes [Refs. A1,A2].

Unsteady forcing of the cascade vanes was established through vortex shedding from a row of five circular cylinders, aligned parallel with the span direction of the vanes and located either upstream or downstream of the vane row. Figure A1 shows the cylinders located at a position 0.8 chords downstream of the vane row and at the midpassage of the vanes (the rods could be positioned at any relative-passage location). Figure A1 also shows three alternate streamwise locations for the forcing-cylinder row, 0.8 and 1.6 chord upstream of the leading edges of the vanes, and 1.6 chords downstream of the trailing edges of the vane-row. In what was fortunate for that cascade configuration, no active control of the cylinder shedding was used, all five cylinders shed in phase and the shedding frequency could be varied by changing the diameter of the cylinders; over the range of Reynolds numbers used in the experiments, the Strouhal number was constant at approximately 0.2, thus the reduced frequency for the von Karman shedding was determined by selecting the rod diameter. All results reported here were for forcing produced off of 3/16 inch diameter rods which yielded a reduced frequency based on the vane half chord of approximately 5 over the entire range of Mach numbers tested; a reduced frequency of 5 yielded primary forcing frequencies at the highest Mach numbers of approximately 9 KHz and the first harmonic at 18 KHz. All unsteady pressure measurements were triggered by the signal from a transducer embedded in one of the forcing cylinders. For further details see [Refs. A1,A2].

A total of 16 stator vanes were instrumented with two surface-mounted Kulite XCS-062 ultraminiature transducers, to provide the two, engine-axis radial positions shown in Figure A2. In addition, four other vanes were instrumented with pressure ports leading to a scanivalve pressure transducer at the two engine-axis, locations and a cascade-axis. Kulite locations were at 7, 12, 20, 30, 40, 50, 65 and 80 percent chord on both the suction and pressure sides of the vanes.

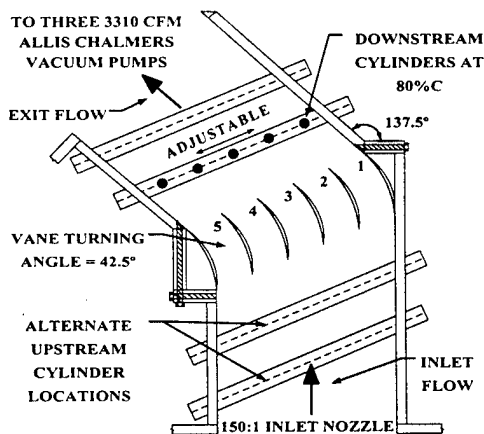


Figure A1. Top View of Mid-1990 Cascade Test Section

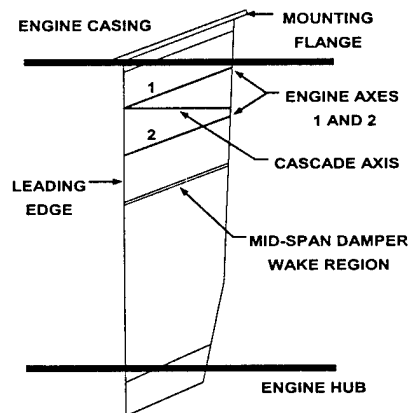


Figure A2. Side View of Stator/Turning Vane

Rearward-Forced Results. Prior to discussing the rearward-forced results, the importance of the rearward-forced data should be pointed out. Although it is our understanding that non-open-literature testing may have been performed, an extensive literature search at the time these tests were being performed found only one other experimental study that considered forcing from downstream [Ref. A3]. This sole other example was not only very low Mach number, but also combined the downstream forcing with upstream forcing at the same time. Further, this previous study drew essentially no conclusions regarding the importance of the rearward forcing, since the upstream and downstream blade counts were identical. Thus, to our knowledge, the results that we published at the time and will be discussed below were the first such results available in the open literature.

Unsteady and time-averaged pressure data were collected at inlet Mach numbers ranging from 0.427 to 0.50, the highest inlet Mach number resulted in a maximum Mach number over the suction side of the vanes of 0.73. Each Mach-number study yielded phase-locked, time-resolved, pressure data like those shown in Figure A3 for the 0.427-inlet-Mach-number, rearward-forced case. Each data trace is the result of 400 ensembles of forcing-cylinder-triggered data records (for details see [Refs. A1,A2]), and only the fluctuating component of the pressure is shown (i.e., the time-averaged pressure has been subtracted from the unsteady pressure trace). Each trace from a particular chord location has been shifted upward on the P/P_{max} axis by two units, in order, from the trailing-edge-near position to the leading-edge-near position; also shown in Figure A3 is the trigger signal. The normalizing amplitudes for the data are 0.843 psi and 0.662 psi for the suction surface and pressure surface, respectively. The raw RMS unsteady pressures in psi, for each of four Mach-number cases ranging from inlet Mach numbers of 0.427 to 0.5, are shown in Figure A4.

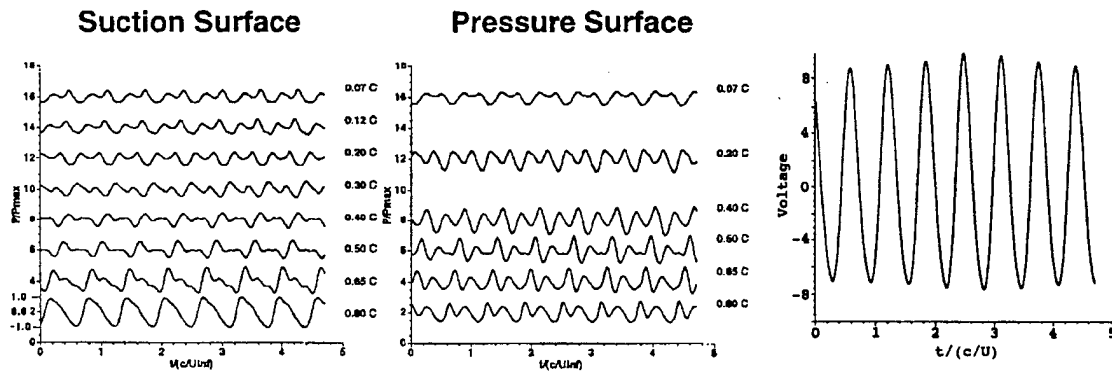


Figure A3. Signals for $M = 0.427$ with Rods 0.8 Chord Aft of Vane Row and Trigger Signal

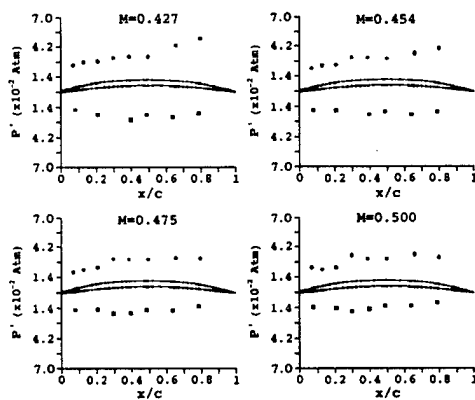


Figure A4. RMS Unsteady Pressure Response With Rods Aft of Vane Row

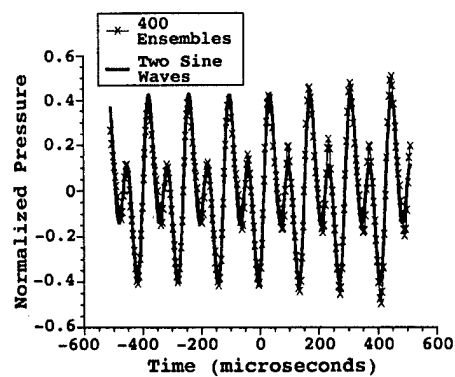


Figure A5. Two Sine Wave Representation

In order to further study the data, each trace was disassembled into its primary (forcing frequency) part and its harmonic part; a representative two-frequency construction at one location for an inlet Mach number of 0.427, is shown in Figure A5 [Refs. A1,A2]. The entire inlet-Mach-0.427 data, represented by four parameters for each location, are given in Table A1.

Table A.1 Amplitude and Phase for Mach 0.427 Data, Primary Frequency = 7,280 Hz

x/c Position	A_p (psi)	ϕ_p (rad)	A_h (psi)	ϕ_h (rad)	RMS Error (psi)
0.07 Suction	0.183	2.415	0.189	-11.907	0.054
0.12 Suction	0.179	2.874	0.217	-10.867	0.056
0.20 Suction	0.158	4.256	0.234	-8.886	0.039
0.30 Suction	0.183	5.645	0.230	-7.747	0.043
0.40 Suction	0.180	6.696	0.243	-4.911	0.064
0.50 Suction	0.200	7.921	0.237	-3.319	0.075
0.65 Suction	0.412	9.441	0.257	0.067	0.014
0.80 Suction	0.751	10.112	0.198	1.476	0.074
0.07 Pressure	0.184	2.625	0.138	-12.398	0.023
0.20 Pressure	0.142	4.026	0.331	-9.528	0.050
0.40 Pressure	0.159	4.703	0.455	-6.950	0.045
0.50 Pressure	0.115	4.981	0.317	-5.101	0.123
0.65 Pressure	0.112	4.692	0.337	-3.394	0.114
0.80 Pressure	0.184	4.389	0.267	-1.714	0.091

With the data in the form of Table A1, it is possible to examine specific aspects of the data. Separate plots of the primary and harmonic components of the unsteady pressures can be made, for example; Figure A6 shows plots for the primary-frequency components. Also shown in Figure A6 are lines indicating the phase delay from near-trailing-edge locations forward on both the suction and pressure surfaces.

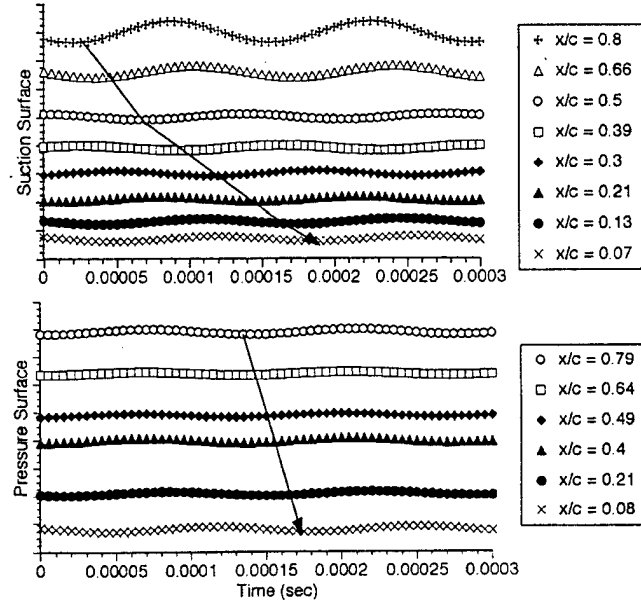


Figure A6. Primary-Frequency Component Time Series

Phase Information. In order to better understand the quality and significance of the data, a simple model was developed for an unsteady disturbance associated with the primary frequency caused by von Karman shedding off the forcing rods, where the disturbance propagates upstream into an undisturbed flow. As the von Karman street sheds into the wake of the cylinder, it produces bound circulation on the cylinder that is equal and opposite to the shed circulation of the alternating-sense vortices in the wake; thus this bound alternating circulation might be represented by a cylinder in a uniform flow with a sinusoidal, fluctuating bound circulation. In incompressible flow, sufficiently far upstream (i.e., $r \gg a$) and along a ray directly upstream from the cylinder,

$$\tilde{V}_{\text{incomp}}(r,t) \cong -V_{\infty} \hat{r} - \frac{\Gamma}{2\pi r} \sin(\omega t) \hat{\theta} \quad (\text{A1})$$

In compressible flow, the apparent distance that the rod is from an upstream location, r , when traveling into an oncoming flow is lengthened as

$$d_{\text{apparent}} = \frac{r}{\sqrt{1 - M_{\infty}^2}} \quad (\text{A2})$$

Further, the signal experiences a time delay which exhibits itself as a phase lag dependent on the frequency, ω , the distance, the speed of sound, and the Mach number, so that in a compressible flow the velocity fluctuation due to the alternating bound circulation in a compressible flow a distance r directly upstream from the cylinder would be

$$\bar{V}_{\text{comp}}(r,t) \cong -V_{\infty} \hat{r} - \frac{\Gamma \sqrt{1 - M_{\infty}^2}}{2\pi r} \sin\left[\omega t - \frac{r\omega}{a_{\infty}(1 - M)}\right] \hat{\Theta} \quad (\text{A3})$$

Using the phase lag of the emanating primary signals, the phase may be linearized to first order in terms of a single "free-stream" Mach number as:

$$\sin\left[\omega t + \phi - \frac{(c - x)\omega}{a_{\infty}(1 - M_{\infty})}\right] \quad (\text{A4})$$

where ϕ is the phase delay at the vane trailing edge, a_{∞} and M_{∞} are the nominal "free-stream" speed of sound and Mach number over the vane surface. Figures A7 and A8 show curves of the phase lag for the primary and harmonic frequencies on the suction and pressure surfaces, respectively.

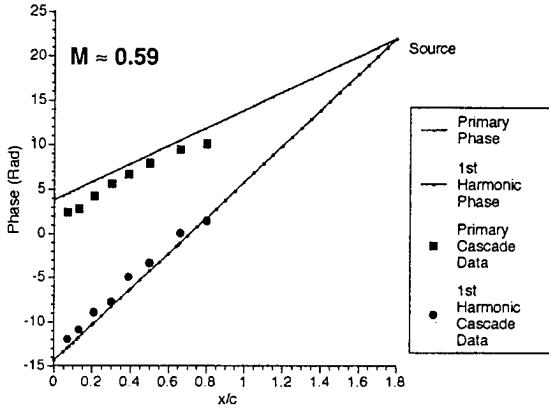


Figure A7. Suction-Surface Phase vs Chord Position for Primary and Harmonic Frequencies

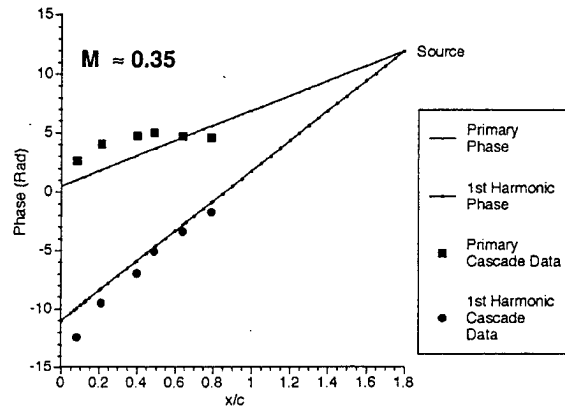


Figure A8. Pressure-Surface Phase vs. Chord Position for Primary and Harmonic Frequencies

The overlaid curves in Figures A7 and A8 are the position-dependent phase delays from Eq. (A4) assuming nominal "free-stream" Mach numbers for the suction and pressure surfaces of 0.59 and 0.35, respectively. These "best-fit" Mach numbers are in excellent agreement with the Mach numbers derived from the time-averaged pressure data over the suction and pressure surfaces of the vanes using

$$M_L = \sqrt{\frac{2}{\gamma - 1} \left[\left(\frac{P_o}{P_L} \right)^{\frac{\gamma - 1}{\gamma}} - 1 \right]} \quad (\text{A6})$$

A plot of the local Mach numbers, M_L , is given in Figure A9. Figures A7 and A8, the agreement with the Mach numbers in Figure A9, similar agreement for all the inlet-Mach-number cases studied, verified that our data was *good* and that the forcing method produced acoustically-propagating, potential disturbances that subsequently interacted with the vane surfaces to yield relatively-large unsteady pressure responses.

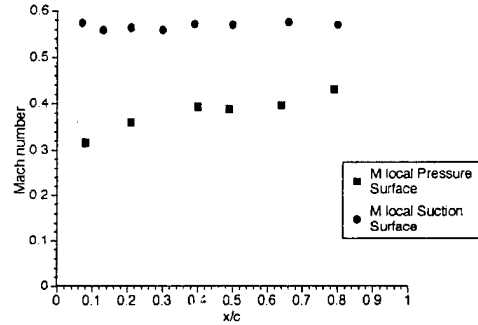


Figure A9. Local Mach Number vs Chord Position

Amplitude Information. Along with being able to examine the disassembled data (like those of Table A1) for phase information, amplitude information could also be examined; the amplitude at the primary forcing frequency for the four Mach-number cases is shown in Figure A10 [Ref. A1]. These data may be compared with the raw RMS data of Figure A4, and it is clear that a more-descriptive picture emerges. *There are two important characteristics of the amplitude data that are of interest to us: first, although we only have data out to the 0.8 chord location, extrapolation of the data to the trailing edge suggests an unsteady-pressure singularity; second, an amplification of the unsteady pressure near the 0.3 x/c location on the suction surface appears to be increasing with Mach number.*

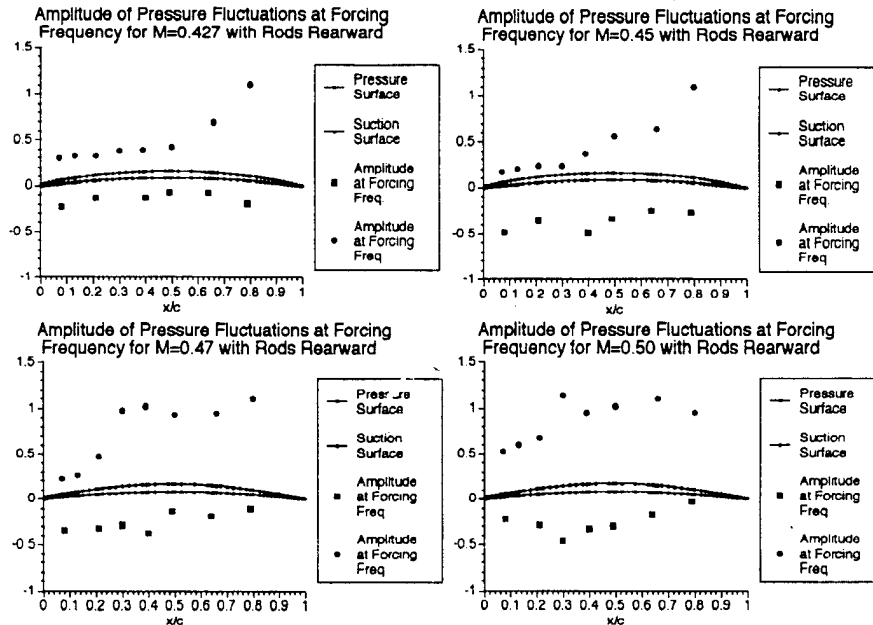


Figure A10. Normalized Pressure Amplitude for Primary Frequency with Increasing Mach Number

The suggestion of a trailing-edge singularity is, as far as we know, the first to have been seen with detailed data, and as detailed in the main body of this proposal, raised the question as to whether or not such a singularity can exist. Until we produced these data, it had been generally accepted that a trailing-edge singularity had been theoretically forbidden, as it most certainly is for waves entering from upstream; however, extensive discussions with Glegg [Ref. A4] and review of the literature (see for example [Ref. A5]), now suggest that such a singularity is probably not forbidden. Clearly, if such a singularity is present in the case of acoustically-propagating, forward traveling waves, this is of first-order importance to the rotor/stator and stage-to-stage interaction problems. *An interesting theoretical point raised in Ref. A5 concerns the presence or absence of a trailing-edge shear layer because these authors draw a distinction in terms of the unsteady pressure response. In terms of cascade*

configurations, an unloaded vane row would produce no shear layer while a loaded vane row would produce a shear layer.

The amplification of the unsteady pressure near the $x/c = 0.3$ location may also be of first-order importance. Atassi, Fang and Ferrand [Ref. A6] had previously predicted the occurrence of this amplification in their theory of "acoustic blockage." According to the theory, acoustic waves traveling forward from the trailing-edge region of a vane row are impeded from progress by the oncoming flow. As this subsonic flow builds in Mach number, depending on the frequencies and wavelengths, the waves can coalesce and amplify the disturbance; amplifications of up to 20 times are theoretically possible as the subsonic Mach number approaches 0.99. The amplification noted in Figure A10 is at the maximum Mach number location; our maximum Mach number was 0.73. We believe that our data provides the first evidence that this mechanism exists and is important even at relatively low Mach numbers, becoming noticeable for maximum Mach numbers as low as 0.6. It should be noted that prior to Atassi's work, unsteady pressure rises near the maximum Mach number region had always been assumed to be associated with transonic flows and oscillating shocks; acoustic blockage provides a fully-subsonic mechanism for providing similar-order amplification for forward-propagating disturbances.

REFERENCES FOR APPENDIX

- A1. Fabian, M.K., Falk, E.A. and Jumper, E.J., "Upstream-Propagating Potential Disturbances Interacting with a Compressible Cascade," *Journal of Propulsion and Power*, **17** (2), 2001, pp. 240-247.
- A2. Fabian, M.K. and Jumper, E.J., "Rearward Forcing of an Unsteady Compressible Cascade," *Journal of Propulsion and Power*, **15**(1), Jan/Feb 1999, pp. 23-30.
- A3. Schmidt, D.P. and Okiishi, T.H., "Multistage Axial-Flow Turbomachine Wake Production, Transport, and Interaction," *AIAA Journal*, **15**, 1977, pp. 1138-1145.
- A4. Glegg, S.A.L., personal communication, at the University of Notre Dame, 8 Nov 1995.
- A5. Crighton, D.G. and Leppington, F.G., "Radiation Properties of the Semi-Infinite Vortex Sheet: the Initial-Value Problem," *Journal of Fluid Mechanics*, **64**, part 2, 1974, pp. 393-414.
- A6. Atassi, H.M., Fang, J. and Ferrand, P., "A Study of the Unsteady Pressure of a Cascade Near Transonic Flow Condition," ASME paper number 94-GT-476, International Gas Turbine and Aerospace Congress and Exposition, The Hague, Netherlands, 1994.

APPENDIX B

Personnel Supported

Eric J. Jumper	Professor, Principal Investigator
Asad Asghar	Graduate Research Assistant (Full Grant)
Eric A. Falk	Graduate Research Assistant (3 Months)
Aleksander Šekularac	Graduate Research Assistant (6 Months)

Publications

Fabian, M.K., Falk, E.A. and Jumper, E.J., "Upstream-Propagating Potential Disturbances Interacting with a Compressible Cascade," *Journal of Propulsion and Power*, **17** (2), March-April 2001, pp. 240-247.

Fabian, M.K. and Jumper, E.J., "Rearward Forcing of an Unsteady Compressible Cascade," *Journal of Power and Propulsion*, **15** (1): 23-30, 1999.

Falk, E.A., Jumper, E.J., Fabian, M.K. and Stermer, J., "Upstream-Propagating Potential Disturbances in the F109 Turbofan Engine Inlet Flow," *Journal of Propulsion and Power*, **17** (2), March-April 2001, pp. 262-269.

Sekularac, A., Falk, E.A. and Jumper, E.J., "A Conformal Mapping Analysis of Cascade Trailing-Edge Flows," AIAA Paper 2000-0229, January 2000.

Wade, P.C., P. I. King, D. R. Hopper, E. J. Jumper and A. Asghar, "Velocity Fields Upstream of Rods Used for Forcing Unsteady Compressible Cascades," AIAA paper 00-3229, July 2000.

Asghar, A., Falk, E.A., Jumper, E.J., Hopper, D.R. and King, P.I., "Unsteady Pressure Response on a Rearward-Forced, Isolated Compressible-Cascade Vane," AIAA Paper 2000-3228, July 2000.

Principal Investigator

ERIC J. JUMPER, Professor

Department of Aerospace and Mechanical Engineering

University of Notre Dame

Notre Dame, IN 46556

Telephone: (574) 631-7680, jumper.1@nd.edu

EDUCATION

Ph.D., Fluid Dynamics and Laser Physics, Air Force Institute of Technology, 1975

M.S., Mechanical Engineering, University of Wyoming, 1969

B.S., Mechanical Engineering, University of New Mexico, 1968

PROFESSIONAL EXPERIENCE

Present Position (since August 1989)	Professor, Department of Aerospace and Mechanical Engineering, University of Notre Dame
Aug 2000 to Jun 2001	Distinguished Visiting Professor, Department of Aeronautics, United States Air Force Academy
July 1987 to July 1989	Chief, Laser Devices Division, Advanced Radiation Technology Office, Air Force Weapons Laboratory, Kirtland AFB, New Mexico
July 1981 to July 1987	Professor, Department of Aeronautics and Astronautics, Air Force Institute of Technology, Dayton, Ohio.
July 1976 to July 1981	Associate Professor, Department of Aeronautics, United States Air Force Academy, Colorado.
January 1974 to July 1976	Research Aerodynamicist, Theoretical Branch, Air Force Weapons Laboratory, Kirtland AFB, New Mexico
September 1969 to June 1972	Research Mechanical Engineer, Flight Environments Branch, 6570th Aerospace Medical Research Laboratory, Wright-Patterson AFB, Ohio.

EXPERIENCE IN AREA OF UNSTEADY AERODYNAMICS AND TUBOMACHINERY

Dr. Jumper has been active in Unsteady Aerodynamics since the late 1970's when he was on the faculty in the Department of Aeronautics, US Air Force Academy. In the early 1980's Dr. Jumper advised six Masters theses at the Air Force Institute of Technology in the area of incompressible unsteady aerodynamics and later advised two Masters theses and a PhD Dissertation in this area at the Notre Dame. In that work many innovative experimental and theoretical techniques were applied to the problem that have extensively influenced and been referenced by others working in the field. These efforts led to 6 journal articles and a host of technical meeting papers. More recently, starting in 1995, Dr. Jumper began working in cascade and engine compressible unsteady aerodynamics. His work has led to a number of new findings that have suggested the important role potential disturbances play in unsteady forced response. These efforts have had a significant effect on the work of others in the field and have led to a number of journal articles with a number more in process. The list below of relevant publications related to this area represents a small subset of over 100 publications credited to Dr. Jumper.

RELEVANT PUBLICATIONS

- Kirk, J. F., Falk, E. A., Jumper, E. J. and Haven, B. A., "Unsteady Forcing of an IGV Forward of a Fan in Subsonic Flow: Phase Results," AIAA Paper no. 2001-3474, July, 2001.
- Falk, E. A., J. F. Kirk, E. J. Jumper, and B. A. Haven, "Unsteady Forcing of an IGV Forward of a Fan in Subsonic Flow: Amplitude Results," AIAA Paper no. 2001-3475, July, 2001.
- Fabian, M.K., Falk, E.A. and Jumper, E.J., "Upstream-Propagating Potential Disturbances Interacting with a Compressible Cascade," *Journal of Power and Propulsion*, **17** (2), 2001, pp. 240-247.
- Fabian, M.K. and Jumper, E.J., "Rearward Forcing of an Unsteady Compressible Cascade," *Journal of Power and Propulsion*, **15** (1): 1999, pp. 23-30.
- Falk, E.A., Jumper, E.J., Fabian, M.K. and Stermer, J., "Upstream-Propagating Potential Disturbances in the F109 Turbofan Engine Inlet Flow," *Journal of Propulsion and Power*, **17** (2), March-April 2001, pp. 262-269.
- Rennie, R.M. and Jumper, E.J., "Experimental Measurements of Dynamic Control-Surface Effectiveness," *Journal of Aircraft*, **33** (5), September-October 1996, pp. 880-887.
- Jumper, E. J. and Hugo, R. J., "Loading Characteristics of Finite Wings Undergoing Rapid Unsteady Motions: A Theoretical Treatment," *Journal of Aircraft*, **31**, May-June 1994, pp. 495-502.
- Jumper, E. J. and Hugo, R. J., "Simple Theories of Dynamic Stall That Are Helpful in Interpreting Computational Results," *Computer Physics Communications*, **65**, 1991, pp. 158-163.
- Jumper, E. J., Dimmick, R. L. and Allaire, A. J. S., "The Effect of Pitch Location on Dynamic Stall," *Fluids Engineering*, **111**, Sept. 1989, pp. 256-262.
- Jumper, E.J., Schreck, S.J. and Dimmick, R.L., "Lift-Curve Characteristics for an Airfoil Pitching at Constant Rate," *Journal of Aircraft*, **24**, October 1987, pp. 680-687.
- Daley, D.C. and Jumper, E.J., "Experimental Investigation of Dynamic Stall for a Pitching Airfoil," *Journal of Aircraft*, **21**, October 1984, pp. 831-832.
- Falk, E.A., Jumper, E.J., Fabian, M.K. and Haven, B.A., "A Characterization of the Unsteady Velocity Field Aft of the F109 Turbofan Rotor," AIAA 99-0237.
- Falk, E.A., Jumper, E.J. and Fabian, M.K., "Upstream Propagating Potential Waves in the F109 Turbofan Engine Inlet Flow," AIAA paper 98-3294, July 1998.
- Falk, E.A., Jumper, E.J. and Fabian, M.K., "An Experimental Study of Unsteady Forcing in the F-109 Turbofan Engine," AIAA paper 97-3286, July 1997.
- Rennie, R.M. and Jumper, E.J., "A Case for Pseudo-Steady Aerodynamic Behaviour at High Motion Rates," AIAA paper 97-0617, January 1997.
- Fabian, M.K. and Jumper, E.J., "Upstream-Propagating Acoustic Waves Interacting with a Compressible Cascade," AIAA paper 97-0380, January 1997.
- Fabian, M.K. and Jumper, E.J., "Convected and Potential Unsteady Disturbances Interacting with an Unsteady Cascade," AIAA paper 96-2672, July 1996.
- Rennie, R. M. and Jumper, E. J., "Dynamic Leading-Edge Flap Scheduling," AIAA paper 95-1904, 1995.
- Fabian, M. K. and Jumper, E. J., "Unsteady Pressure Distributions Around Compressor Vanes in an Unsteady, Transonic Cascade," AIAA paper 95-0302, 1995.
- Rennie, R.M. and Jumper, E.J., "Experimental Measurements of Dynamic Control Surface Effectiveness," AIAA paper 94-0504, 1994.
- Hugo, R. and Jumper, E., "Controlling Unsteady Lift Using Unsteady Trailing-Edge Flap Motions," AIAA paper 92-0275, January 1992.
- Jumper, E. J. and Hugo, R. J., "Loading Characteristics of Finite Wings Undergoing Rapid Unsteady Motions: A Theoretical Treatment," AIAA paper 91-3263, September 1991.
- Jumper, E. J., Merritt, P., Lamberson, S., Gates, G., and Bertin, J. J., "Time-Resolved Force and Moment Measurements on a Cubic Body in Cross Flow: Implications to Wind-Induced Jitter of Telescopes," AIAA paper 91-0554.
- Jumper, E. J., "Simple Theories of Dynamic Stall That Are Helpful in Interpreting Computational Results," *Proceedings of the IMACS 1st International Conference on Computational Physics*, Association Internationale Pour Les Mathematiques et Calculeteurs en Simulation, pp. 240-243, June 1990.
- Jumper, E.J., Dardis, W.J. and Stephen, E.J., "Toward an Unsteady-Flow Airplane," AIAA Paper Number AIAA-88-0752, 1988.
- Jumper, E.J., and Stephen, E.J., "Toward Unsteady Lift Augmentation: An Assessment of the Role of Competing Phenomena in Dynamic Stall," *Proceedings of the Second AFOSR Workshop on Unsteady Separated Flows*, U.S. Air Force Academy, Colorado, July 1987.

- Jumper, E.J., Dimmick, R.L. and Allaire, A.J.S., "The Effect of Pitch Location on Dynamic Stall," *Forum on Unsteady Flow Separation*, FED-Vol. 52, ASME, June 1987, pp. 201-208.
- Jumper, E.J., Hitchcock, J.E., Lawrence, T.S. and Doeken, R.G., Jr., "Investigating Dynamic Stall Using a Modified Momentum-Integral Method," AIAA Paper Number AIAA-87-0431, 1987.
- Jumper, E.J., "Mass Ingestion: A Perturbation Method Useful in Analyzing Some Boundary-Layer Problems," ASME Paper No. ASME-86-WA/FE-10, 1986.
- Jumper, E.J., Schreck, S.J. and Dimmick, R.L., "Lift-Curve Characteristics for an Airfoil pitching at Constant Rate," AIAA Paper Number AIAA-86-0117, 1986